


Non-Markovian transient spectroscopy in cavity QED

Z. McIntyre^{*} and W. A. Coish[†]

Department of Physics, McGill University, 3600 rue University, Montreal, Quebec H3A 2T8, Canada

 (Received 4 June 2022; revised 12 August 2022; accepted 14 October 2022; published 30 November 2022)

We theoretically analyze measurements of the transient field leaving a cavity as a tool for studying non-Markovian dynamics in cavity quantum electrodynamics (QED). Combined with a dynamical decoupling pulse sequence, transient spectroscopy can be used to recover spectral features that may be obscured in the stationary cavity transmission spectrum due to inhomogeneous broadening. The formalism introduced here can be leveraged to perform *in situ* noise spectroscopy, revealing a robust signature of quantum noise arising from noncommuting observables, a purely quantum effect.

DOI: [10.1103/PhysRevResearch.4.L042039](https://doi.org/10.1103/PhysRevResearch.4.L042039)

Introduction. Significant effort has recently gone towards reaching the strong-coupling regime of cavity quantum electrodynamics (QED) for individual long-lived spin and charge qubits, with the goals of achieving long-range coupling [1], performing fundamental studies of many-body phenomena [2], and realizing other exotic effects arising from hybrid systems [3]. Strong coupling has been observed between microwave photons and charge qubits in GaAs [4], spin qubits in silicon [5–7], resonant-exchange qubits in GaAs triple quantum dots [8], and spin qubits in carbon nanotube double quantum dots [9,10] (DQDs). Two-qubit, photon-mediated interactions have been observed between charge qubits in GaAs DQDs [11] and between spin qubits in silicon DQDs [12,13]. As these devices reach a progressively higher level of sophistication and quality, it is increasingly important to characterize the qubits and their local environments *in situ*, together with the components that define the cavity.

In-situ characterization of a two-level emitter (qubit) coupled to a cavity is often done by measuring a transmission or reflection spectrum [4,5,7,14–16] in a setup similar to that shown in Fig. 1. In this setup, an input tone $r_{\text{in},1}(t) = (2\pi)^{-1} \int d\omega e^{-i\omega t} r_{\text{in},1}(\omega)$ is introduced, and after a time long compared to the cavity decay time κ^{-1} , the output field $r_{\text{out},2}(t)$ reaches a steady state. The stationary transmission $A_{\Gamma}(\omega) = r_{\text{out},2}(\omega)/r_{\text{in},1}(\omega)$ then carries information about the qubit accounting for its interaction with the environment and resulting decay processes. To interpret the transmission, it is common to make the simplifying assumption that the qubit dynamics are generated by a Markovian master equation, with parameters characterizing dephasing and relaxation rates. The standard tools of input-output theory [16–19] can then be

applied. The Markovian assumption is often an excellent approximation for single-atom emitters [14,15] and for the superconducting transmon qubits commonly used in circuit QED [16]. With some exceptions [20,21], these systems typically have coherence times T_2 limited by the exponential energy relaxation time T_1 : $T_2 \simeq 2T_1$. In stark contrast, spin and charge qubits defined using semiconductor nanostructures almost universally undergo nonexponential (non-Markovian) pure dephasing on a time scale $T_2^* \ll T_1$ arising from inhomogeneous broadening due to low-frequency charge noise or slow nuclear-spin environments. A different approach is required for these and many other non-Markovian systems.

A dynamical decoupling pulse sequence can help mitigate the effects of strong inhomogeneous broadening, but the result is a train of manifestly non-Markovian collapses and revivals (echoes) in qubit coherence. Although these revivals (of duration $\sim T_2^*$) can be mapped to the transient output field $r_{\text{out},2}(t)$ (see Fig. 1), their effect on the stationary transmission spectrum is negligible since they are, by definition, transient. Similar revivals have already been exploited for measurement in spin-echo experiments on ensembles [22,23]. For a low- Q resonator, the relationship between spin coherence and the output field is relatively simple and time local [22]. By contrast, it is a nontrivial problem to relate the complex pattern of revivals arising from, e.g., a dynamical decoupling sequence, to real-time non-Markovian coherence dynamics for a high- Q cavity. We perform this analysis here. Although our focus is on individual spin and charge qubits under a widely used dynamical decoupling sequence, the ideas presented here are generally applicable to ensembles and to a wide range of non-Markovian systems in cavity QED, a topic of significant recent interest [24–28].

Model. We start from a typical cavity-QED setup (see Fig. 1), with dynamics governed by the quantum master equation (taking $\hbar = 1$):

$$\dot{\rho} = -i[H(t), \rho] + \frac{\gamma_{\phi}}{2} \mathcal{D}[\sigma_z]\rho + \kappa_{\text{ext}} \mathcal{D}[a]\rho. \quad (1)$$

Here, $\rho = \rho(t)$ is the joint state of the qubit, cavity, quantum environment, and transmission lines. The qubit (with Pauli

*zoe.mcintyre@mail.mcgill.ca

†coish@physics.mcgill.ca

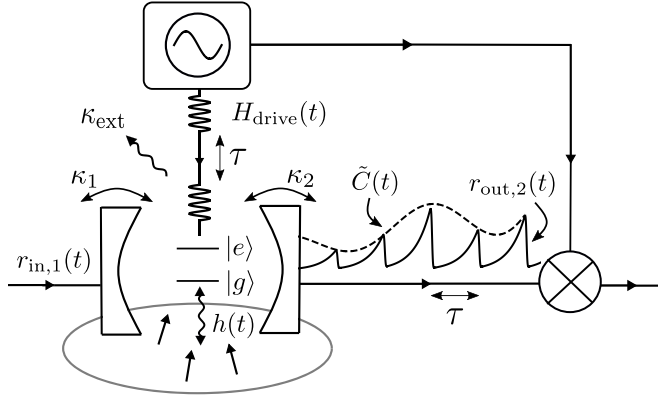


FIG. 1. A typical cavity-QED setup. The transmission spectrum is obtained from the linear response of the output signal $r_{\text{out},2}(t)$ to a monochromatic input tone, $r_{\text{in},1}(t)$. In contrast, the transient spectrum is found, for $r_{\text{in},1}(t) = 0$, by generating a sequence of control pulses via a qubit drive $H_{\text{drive}}(t)$. These pulses induce non-Markovian coherence revivals with envelope $\tilde{C}(t)$ for a qubit coupled to its environment through some interaction $h\sigma_z/2$. A phase-sensitive measurement of $r_{\text{out},2}(t)$ can then be used to determine $\tilde{C}(t)$. The decay rates at the input and output ports of the cavity are denoted κ_1 and κ_2 , respectively, while extrinsic decay is denoted κ_{ext} .

operator $\sigma_z = |e\rangle\langle e| - |g\rangle\langle g|$ undergoes Markovian pure dephasing at a rate γ_ϕ , while photons in the cavity mode (annihilated by a) decay at an extrinsic rate κ_{ext} . The damping superoperator acts like $\mathcal{D}[\mathcal{O}]\rho = \mathcal{O}\rho\mathcal{O}^\dagger - \{\mathcal{O}^\dagger\mathcal{O}, \rho\}/2$ for any operator \mathcal{O} ; in addition to damping processes, the density operator ρ evolves under the Hamiltonian

$$H(t) = \frac{1}{2}[\Delta + \Omega(t)]\sigma_z + \frac{1}{2}h(t) + \omega_c a^\dagger a + g\sigma_x(a + a^\dagger) + H_{\text{drive}}(t) + \sum_{i=1,2} \sum_k (\lambda_{k,i} e^{i\omega_k t} r_{k,i}^\dagger a + \text{H.c.}), \quad (2)$$

where Δ is the qubit resonance frequency, ω_c is the cavity frequency, and g is the qubit-cavity coupling. The term $H_{\text{drive}}(t)$ describes a drive acting on the qubit, while noise is generated by $\Omega(t) = \eta(t) + h(t)$, where $\eta(t)$ is a classical noise parameter and $h(t) = e^{i(H_E - h/2)t} h e^{-i(H_E - h/2)t}$ acts on the environment alone. The time dependence of $h(t)$ arises from a laboratory-frame Hamiltonian $H_E + h\sigma_z/2$ together with the assumption that the environment is prepared in a steady state while coupled to the qubit held in $|g\rangle$ (see below and Ref. [29]). We take $\eta(t)$ to be generated by a stationary Gaussian process with zero mean ($\langle\langle\eta(t)\rangle\rangle = 0$) and spectral density

$$S_\eta(\omega) = \int dt e^{-i\omega t} \langle\langle\eta(t)\eta(0)\rangle\rangle, \quad (3)$$

where here, the double angle brackets $\langle\langle\rangle\rangle$ represent an average over noise realizations. The terms $\propto \lambda_{k,i}$ in Eq. (2) describe coupling of the cavity mode to the input (output) [for $i = 1(2)$] transmission-line mode annihilated by $r_{k,i}$ and having frequency ω_k . For modes propagating in one dimension, $r_{\text{in},i}(t) = [c/L]^{1/2} \sum_k e^{-i\omega_k t} \langle r_{k,i} \rangle_0$ and $r_{\text{out},i}(t) = [c/L]^{1/2} \sum_k \langle r_{k,i} \rangle_t$, where L is the length of the transmission line and c is the speed of light. The notation $\langle\langle\mathcal{O}\rangle\rangle_t$ indicates

an average with respect to the state $\rho(t)$, together with an average over realizations of the classical noise $\eta(t)$: $\langle\langle\mathcal{O}\rangle\rangle_t = \langle\langle\text{Tr}\{\mathcal{O}\rho(t)\}\rangle\rangle$.

Transient spectroscopy. In order to accurately monitor qubit dynamics through the transient output field $r_{\text{out},2}(t)$, we consider the following protocol: (i) An undriven single-sided ($\kappa_1 = 0$) cavity is prepared in a vacuum state $|0\rangle$ far detuned from (or decoupled from) the qubit. (ii) The qubit is prepared in its ground state $|g\rangle$, and the environment is allowed to reach a steady state $\bar{\rho}_E$ in contact with the qubit: $[H_E - h/2, \bar{\rho}_E] = 0$. (iii) At $t = 0$, the qubit and cavity are tuned close to resonance (or the coupling g is turned on), and a finite drive $H_{\text{drive}}(t \geq 0)$ generates qubit coherence $\langle\sigma_x\rangle_t$. This coherence is related to the cavity field $\langle\tilde{a}\rangle_t = e^{i\Delta t} \langle a \rangle_t$ via direct integration of Eq. (1):

$$\langle\tilde{a}\rangle_t = -ig \int_{-\infty}^{\infty} dt' \chi_c(t-t') e^{i\Delta t'} \langle\sigma_x\rangle_{t'}, \quad (4)$$

where $\chi_c(t) = e^{-i\delta t - \kappa t/2} \Theta(t)$ for a cavity-qubit detuning $\delta = \omega_c - \Delta$ and total cavity decay rate $\kappa = \kappa_{\text{ext}} + \kappa_2$. Neglecting retardation effects, the measured output field is then given by the input-output relation $r_{\text{out},2}(t) = \sqrt{\kappa_2} \langle a \rangle_t$ [17]. For a single cavity-coupled qubit, the protocol [(i)-(iii)] is limited to gathering $\lesssim 1$ bit of information per cycle, similar to many early cavity-QED schemes [14]. These steps must therefore be repeated many times to estimate the expectation value $\langle\sigma_x\rangle_t$.

Dynamical decoupling. For concreteness, we consider an N -pulse Carr-Purcell-Meiboom-Gill (CPMG) sequence, where coherence preparation at $t = 0$ [such that $\langle\sigma_x\rangle_0 = \frac{1}{2} \langle\sigma_x\rangle_0 \neq 0$] is followed by π_x -pulses at times $t = \tau/2, 3\tau/2, \dots, (N-1/2)\tau$, leading to coherence revivals at times $t = n\tau$, $n = 1, 2, \dots, N$ (see the Supplemental Material [29] for the general formalism, valid for other pulse sequences). We further specialize to the regime $g < \kappa \ll \tau^{-1}$, where cavity backaction effects can be treated as a small correction. In this regime, the coherence factor $C(t) = \langle\sigma_x\rangle_t / \langle\sigma_x\rangle_0$ can be written in terms of a comb of revivals (echoes) with peaks $\sim G_n(t - n\tau)$ centered at $t = n\tau$ and an echo envelope $\tilde{C}(t)$:

$$C(t) = \sum_n e^{-i\Delta(t-n\tau)} G_n(t - n\tau) \mathcal{K}^n \tilde{C}(n\tau). \quad (5)$$

Here, $\mathcal{K}z = z^*$ for all $z \in \mathbb{C}$. If $T_2^* \ll \tau$ [where $2/(T_2^*)^2 = (2\pi)^{-1} \int d\omega S_\eta(\omega)$], and if $\tilde{C}(n\tau)$ is slowly varying on the timescale T_2^* , then we find

$$G_n(t) = e^{\sqrt{\gamma_P n \tau} \langle\langle e^{-\Gamma_P(\eta)n\tau/2} e^{-i\eta t} \rangle\rangle}, \quad (6)$$

where $\eta = \eta(0)$ is the low-frequency contribution to $\eta(t)$, $\Gamma_P(\eta) = g^2 \kappa / [(\eta - \delta)^2 + (\kappa/2)^2]$ is the Purcell decay rate at fixed η , and $\gamma_P = (gT_2^*)^2 \kappa/2$. The echo envelope is

$$\tilde{C}(n\tau) = e^{-\sqrt{\gamma_P n \tau} - \gamma_\phi n \tau} \langle\langle \text{Tr}\{U_-^\dagger(n\tau) U_+(n\tau) \bar{\rho}_E\} \rangle\rangle, \quad (7)$$

where $U_\pm(n\tau) = \mathcal{T} \exp\{-\frac{i}{2} \int_0^{n\tau} [h(t') \pm s(t') \Omega(t')]\}$ are evolution operators acting on the environment, conditioned on the σ_z -eigenvalue (\pm) of the qubit. Here, \mathcal{T} is the time-ordering operator and $s(t) = (-1)^{n(t)}$ for $n(t)$ π -pulses having taken place up to time t . For $n < 1/(\gamma_P \tau)$, backaction due to Purcell decay is negligible and the revivals are well approximated by

$G_n(t) \simeq G_0(t) = e^{-(t/T_2^*)^2}$. The effects of backaction will be further discussed below.

Taking the Fourier transform of Eq. (4) gives $\langle \tilde{a} \rangle_\omega = -ig\chi_c(\omega) \langle \sigma_x \rangle_{\omega+\Delta}$; the cavity susceptibility acts as a filter, $\chi_c(\omega) = [i(\delta - \omega) + \kappa/2]^{-1}$. In the high- Q limit ($Q = \omega_c/\kappa \gg 1$), $\chi_c(\omega)$ suppresses the counter-rotating component $\langle \sigma_+ \rangle_t$, allowing us to replace $\langle \sigma_x \rangle_t \simeq \langle \sigma_- \rangle_t = C(t) \langle \sigma_- \rangle_0$ in Eq. (4) for $|\delta| \ll |\Delta|$. Under the assumptions laid out above, we find a general expression relating $\langle \tilde{a} \rangle_\omega$ to the echo envelope $\tilde{C}(n\tau)$ [29]. For a narrow cavity resonance, $\kappa T_2^* \ll 1$, $\langle \tilde{a} \rangle_\omega$ will be sharply peaked around $\omega = \delta$, leading to

$$\langle \tilde{a} \rangle_{\omega=\delta} \simeq -i \langle \sigma_x \rangle_0 \frac{\sqrt{\pi} g T_2^*}{\kappa} \left[\tilde{C}_{N,\tau}(\delta) - \frac{1}{2} C(0) \right], \quad (8)$$

where we neglect corrections smaller by $O(g/\kappa)$, $O(\kappa/\Delta)$. Here,

$$\tilde{C}_{N,\tau}(\omega) = \sum_{n=0}^N e^{in(\omega+\Delta)\tau} \tilde{G}_n \mathcal{K}^n \tilde{C}(n\tau), \quad (9)$$

where $\tilde{G}_n = (\sqrt{\pi} T_2^*)^{-1} \int_{-\infty}^{\infty} dt G_n(t)$. The echo envelope $\tilde{C}(t)$ can thus be reconstructed by measuring $r_{\text{out},2}(\omega)$ to infer $\langle \tilde{a} \rangle_{\omega=\delta}$ over some detuning interval $O(2\pi/\tau)$ and then inverting the discrete Fourier transform $\tilde{C}_{N,\tau}(\omega)$. The revival amplitudes $\mathcal{K}^n \tilde{C}(n\tau)$ depend alternately on $\tilde{C}(n\tau)$ (for n even) and $\tilde{C}^*(n\tau)$ (for n odd); this even/odd alternation is a direct result of the high- Q limit, which (as we now show) can be exploited to identify a purely quantum effect.

Quantum noise. For the secular coupling $h\sigma_z/2$ considered here, we find a generic expression for the echo envelope $\tilde{C}(n\tau)$: Without loss of generality, we take $\langle h \rangle_t = 0$, in which case a Magnus expansion to second order in $h(t)$ followed by a Gaussian approximation (valid for a large uncorrelated environment [30]—see Ref. [31] for the non-Gaussian generalization) gives

$$\tilde{C}(n\tau) \simeq e^{-\sqrt{\gamma} n\tau - \gamma_\phi n\tau} \exp\{-i\Phi_q(n\tau) - \chi(n\tau)\}, \quad (10)$$

where

$$\Phi_q(n\tau) = \int \frac{d\omega}{2\pi} \frac{F_q(\omega, n\tau)}{\omega^2} S_q(\omega), \quad (11)$$

$$\chi(n\tau) = \int \frac{d\omega}{2\pi} \frac{F_c(\omega, n\tau)}{\omega^2} S_c(\omega). \quad (12)$$

Here, $F_c(\omega, n\tau) = (\omega^2/2) |\int_0^{n\tau} dt e^{i\omega t} s(t)|^2$ is the usual filter function for classical noise [32], $F_q(\omega, n\tau) = \omega \int_0^{n\tau} dt \sin(\omega t) s(t)$ is a new quantum-noise filter function, and

$$\begin{aligned} S(\omega) &= S_c(\omega) + iS_q(\omega) \\ &= \lim_{\epsilon \rightarrow 0^+} \int_{-\infty}^{\infty} dt e^{-i\omega t - \epsilon|t|} \langle \Omega(|t|) \Omega \rangle \end{aligned} \quad (13)$$

is the spectral density [29]. The magnitude of $\tilde{C}(n\tau)$ is then determined by the classical part of the noise spectrum $S_c(\omega) = \text{Re}[S(\omega)] = S_\eta(\omega) + S_h(\omega)$, where $S_h(\omega)$ depends only on the symmetrized correlation function $\langle \{h(|t|), h\} \rangle$. For a quantum environment, the envelope $\tilde{C}(n\tau)$ generally has a phase $\Phi_q(n\tau)$ [Eq. (11)] determined by the quantum noise $S_q(\omega) = \text{Im}[S(\omega)]$, due to the antisymmetrized correlation function

$\langle [h(|t|), h] \rangle$ [29]. This phase will manifest itself in the alternation between \tilde{C} and \tilde{C}^* in the discrete Fourier transform in Eq. (8) for n even/odd. The importance of quantum noise due to noncommuting observables has long been recognized in the mesoscopic-physics community [33]. In addition, it has been measured in CPMG experiments performed on nitrogen-vacancy center spin qubits in diamond, leading to a phase shift $\Phi_q(n\tau) \sim \pi$ [34].

Despite this recognition of quantum noise in other communities, a common simplification in noise spectroscopy is to assume a frequency-symmetric, real-valued spectrum, $S(\omega) = S(-\omega) = S^*(\omega)$, as would arise from a classical fluctuating field [35–40] (although quantum noise has been incorporated into some recent theory works [41,42]). By leveraging the sensitivity of the cavity field to the phase of qubit coherence revivals in the high- Q regime [Eq. (8)], we identify a robust even-odd modulation of revivals arising from $S_q(\omega) = \text{Im} S(\omega)$, unique to quantum environments. Notably, this even-odd effect would not appear for coupling of the form $h\sigma_z/2$ when $\bar{\rho}_E$ is stationary with respect to H_E alone ($[H_E, \bar{\rho}_E] = 0$) [41,42], as may occur for an environment prepared in the absence of the qubit. The quantum-noise phase $\Phi_q(n\tau)$ [Eq. (11)] thus appears as a direct consequence of the initial condition, $[H_E - h/2, \bar{\rho}_E] = 0$ [29].

Characterizing a single nuclear spin. As a concrete application, we consider an electron spin qubit in a silicon double quantum dot (DQD) [5–7], exposed to a spatially varying magnetic field. The magnetic field is assumed to have an x component $B_x(\mathbf{r})$ that averages to zero over the DQD and a uniform z component B_z [30], a setup that is commonly used to generate spin-photon coupling [44]. This leads to a secular coupling and “environment” Hamiltonian given by

$$\frac{1}{2} h\sigma_z = \frac{1}{2} A I_z \sigma_z, \quad H_E = \gamma (B_x I_x + B_z I_z). \quad (14)$$

Here, $B_x = B_x(\mathbf{r}_0)$ for a ^{29}Si nuclear spin located at position \mathbf{r}_0 , \mathbf{I} is a spin- I operator ($I = 1/2$ for ^{29}Si), A is the hyperfine coupling, and $\gamma = -5.319 \times 10^7 \text{ rad T}^{-1} \text{ s}^{-1}$ is the gyromagnetic ratio. The same model also applies to a spin qubit in a uniform \mathbf{B} -field, provided the spin has an anisotropic g tensor, leading to noncollinear quantization axes for the qubit and nuclear spin. Alternatively, this model can describe a qubit having a finite charge dipole interacting with the electric field produced by a two-level charge fluctuator, where γB_z and γB_x are replaced by the fluctuator bias and tunnel splitting, respectively [20,45,46].

For an electron-spin qubit in isotopically enriched silicon, coherence times may be limited by a small number of ^{29}Si nuclear spins [47]. Extracting parameters for individual nuclear spins could facilitate decoherence suppression through a notch-filter dynamical decoupling sequence [48], or allow for a transfer of information from the electron spin to the nuclear spin for a long-lived quantum memory. The problem of characterizing the spin state of a single ^{31}P donor nuclear spin (with hyperfine coupling $A/2\pi \approx 25 \text{ MHz}$) was recently considered theoretically in Ref. [49] in the context of transmission spectroscopy (described by input-output theory). For a ^{29}Si nuclear spin coupled to a quantum-dot-bound electron spin, however, the hyperfine coupling is orders of magnitude weaker ($A/2\pi \approx -0.25 \text{ MHz}$ has been measured,

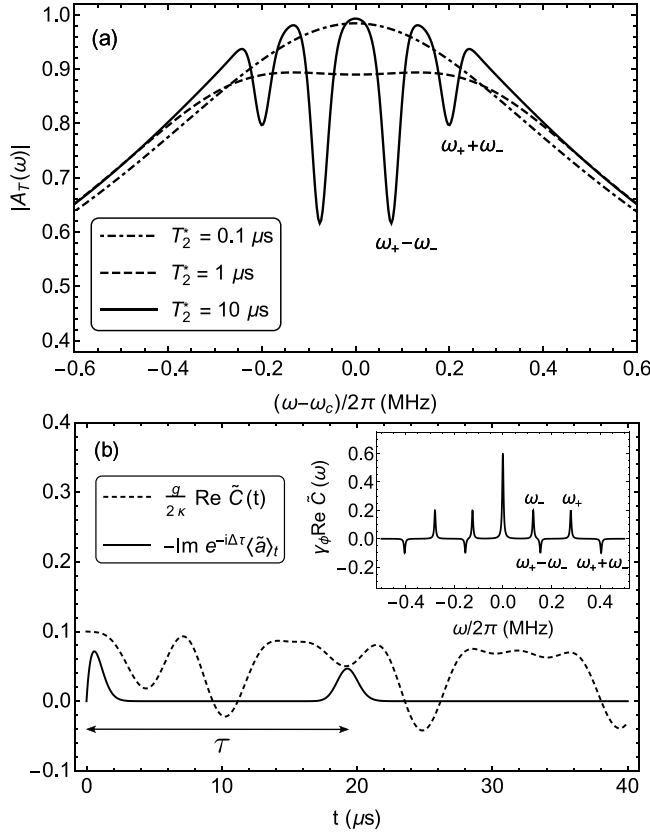


FIG. 2. (a) Inhomogeneously broadened cavity transmission at $\delta = 0$ for three values of T_2^* ($T_2^* = 0.1 \mu\text{s}$, $1 \mu\text{s}$, and $10 \mu\text{s}$). We take $A/2\pi = -0.250 \text{ MHz}$ [43], $\gamma B_z = \gamma B_x = A/2$, $\gamma_\phi^{-1} = 100 \mu\text{s}$, $\kappa/2\pi = 1 \text{ MHz}$, and $g/\kappa = 0.2$. For $B_z = 15 \text{ mT}$, $\omega_c/2\pi = g^* \mu_B B_z/2\pi = 0.4 \text{ GHz}$, where $g^* = 2$. We assume an infinite-temperature initial state for the nuclear spin. (b) Revivals in the cavity field, modulated by the echo envelope, assuming the same parameters as in (a) with $T_2^* = 1 \mu\text{s}$. Once the echo envelope has been mapped out (e.g., by varying τ), it can be Fourier transformed [inset] to recover the frequencies ω_\pm obscured in (a).

for instance [43]). Spectral information in the transmission $A_T(\omega) = \langle\langle A_T(\omega, \eta) \rangle\rangle$ might be entirely obscured due to inhomogeneous broadening as a result [Fig. 2(a)]. Here, we have averaged the transmission $A_T(\omega, \eta)$ for a time-independent but random value of η [29]. Even when spectral information about the nuclear spin is completely obscured in a more conventional measurement of the transmission spectrum, it can still be recovered in the transient spectrum resulting from a spin-echo sequence.

A finite value $B_x \neq 0$ leads to echo envelope modulations following a Hahn-echo sequence (CPMG with $N = 1$). For $\kappa T_2^* > 1$ but $Q = \omega_c/\kappa \gg 1$, the cavity-field revival is modulated by the echo envelope according to $\langle a \rangle_\tau \simeq -i \frac{2g}{\kappa} \tilde{C}(\tau) \langle \sigma_- \rangle_0$ [see Fig. 2(b)]. [In the opposite regime, $\kappa T_2^* < 1$, it is instead modulated according to $\langle a \rangle_\tau \simeq -i \sqrt{\pi} g T_2^* \tilde{C}(\tau) \langle \sigma_- \rangle_0$.] In the case of a single environmental spin, the Gaussian approximation cannot be justified, but this model can be solved exactly: For a fully randomized (infinite-temperature) initial condition for the nuclear spin, the Hahn-echo amplitude at $t = \tau$ is given by $\tilde{C}(\tau) = e^{-\gamma_\phi \tau} [1 -$

$\delta \tilde{C}(\tau)]$, where

$$\delta \tilde{C}(\tau) = 2 \sin^2(\Delta\phi) \sin^2\left(\frac{\omega_+\tau}{4}\right) \sin^2\left(\frac{\omega_-\tau}{4}\right). \quad (15)$$

Here, $\omega_\pm = [(\gamma B_x)^2 + (\gamma B_z \pm A/2)^2]^{1/2}/2$ and $\Delta\phi = \phi_+ - \phi_-$, where $\phi_\pm = \arctan[2\gamma B_x/(2\gamma B_z \pm A)]$. For the infinite-temperature environmental initial condition considered here, $\tilde{C}(\tau)$ is real and there is no quantum-noise contribution. A polarized initial condition would, however, lead to a complex-valued $\tilde{C}(\tau)$, a signature of a quantum environment and of quantum noise [50]. In this illustrative case of coupling to a single spin, the frequencies ω_\pm and angular difference $\Delta\phi$ can be extracted independently from the peak positions and peak heights in a Fourier transform of Eq. (15) [Fig. 2(b), inset], allowing for recovery of both components of the local magnetic field B_x, B_z , and of the local hyperfine coupling A . For the value of A used in Fig. 2, the visibility $\sin^2(\Delta\phi)$ of the echo-envelope oscillations [cf Eq. (15)] is maximized for $B_z = B_x = 15 \text{ mT}$. While this combination of values is possible, it would be fortuitous and would require a relatively low cavity frequency, $\omega_c/2\pi \simeq 0.4 \text{ GHz}$. Away from these values, $\sin^2(\Delta\phi) \simeq [A\gamma B_x/(\gamma B_z)^2]^2$ for $A, \gamma B_x < \gamma B_z$. When $[A\gamma B_x/(\gamma B_z)^2]^2 \ll 1$, the amplitude of the modulations can be enhanced through a large- N CPMG sequence: As is well known, a multi-pulse CPMG sequence can be used to amplify specific Fourier components of the noise [34,38,51]. A noise contribution $S(\omega) \sim |\beta_0|^2 \delta(\omega - \omega_0)$, for instance, leads for $n = N$ to an amplitude $\tilde{C}(N\pi/\omega_0) \simeq e^{-(N/N_0)^2}$, where $N_0 = \sqrt{\pi} \omega_0/(2|\beta_0|)$, giving a visibility $\propto (N/N_0)^2$ that increases with N for $N < N_0$. As N increases, however, the ability to extract information about the qubit coherence may become limited by cavity-induced backaction.

Backaction. A protocol that requires continuous monitoring of a qubit in a driven cavity may suffer from backaction induced by qubit dephasing due to cavity-photon shot noise [52], as well as measurement-induced backaction that necessitates a continuous update of the quantum state [53]. In contrast, the protocol presented here involves no direct cavity driving, and the qubit is repared in each measurement cycle. However, coupling to the cavity will still induce unwanted backaction on the qubit through Purcell decay, beyond the minimum backaction required to extract information about the qubit coherence dynamics: For a CPMG sequence, and for $\kappa\tau \gg 1$, we find that inhomogeneously broadened Purcell decay leads to a stretched-exponential decay, $\tilde{C}(n\tau) \propto e^{-\sqrt{\gamma_P n\tau}}$. For $n > 1/(\gamma_P \tau)$, it also gives rise to a simultaneous broadening (in time) and modulation of the echo revivals,

$$G_n(t) \simeq e^{-\left(\frac{t}{T_2^*}\right)^2} \cos\left[\sqrt{2}(\gamma_P n\tau)^{1/4} \frac{t}{T_2^*}\right], \quad (16)$$

leading to an additional suppression of large- n cavity revivals by a factor $\tilde{G}_n \simeq 2e^{-2\sqrt{\gamma_P n\tau}}$ [29]. This suppression limits the number of revivals (echoes) that can be measured before coherence decays to zero, and hence, the signal that can be extracted in each cycle from measurements on the transmission line.

Coherence is transferred from the qubit to the cavity via Eq. (4), and from the cavity to the output transmission line via $\dot{r}_{k,2}(t) = -i\omega_k r_{k,2}(t) - i\lambda_{k,2} a(t)$. After (i) integrating these equations of motion, (ii) tracing out the cavity, qubit, and environment, and (iii) averaging over realizations of the noise $\eta(t)$, we obtain the reduced density matrix ρ_{TL} of the output transmission line. Provided there is at most one photon in the transmission line (this limit can always be reached by reducing κ_2/κ),

$$\rho_{\text{TL}} = (1 - S)\rho_{\text{inc}} + S|\psi\rangle\langle\psi|, \quad (17)$$

where ρ_{inc} is the incoherent part of the density matrix [$\text{Tr}(r_{k,2}\rho_{\text{inc}}) = 0 \forall k$] and $|\psi\rangle = \frac{1}{\sqrt{2}}(|0\rangle + |1\rangle)$. Here, $|1\rangle = 2S^{-1} \sum_k \langle r_{k,2} | r_{k,2}^\dagger | 0 \rangle$, where $S = 2[\sum_k |\langle r_{k,2} \rangle|^2]^{1/2}$. For $S \rightarrow 1$, information about the qubit coherence dynamics is fully transferred into the pure state $|\psi\rangle$ of a two-level system, allowing, in principle, up to one bit of information to be extracted per measurement cycle. Typically, however, $S \ll 1$ will be realized, yielding $\ll 1$ bit of information per cycle. For example, we find that a Hahn echo sequence (CPMG with $N = 1$) leads to [29]

$$S \leq S_{\text{Hahn}} = \frac{\sqrt{5\pi}}{2} g T_2^* \left(\frac{\kappa_2}{\kappa} \right)^{1/2}, \quad (18)$$

limited by $g T_2^* \ll 1$. For a large- N CPMG sequence, by contrast, we find a significantly larger bound,

$$S \lesssim S_{\text{CPMG}} = \frac{2\sqrt{\pi}}{3} \left[\left(\frac{\kappa_2}{\kappa} \right) \left(\frac{1}{\kappa\tau} \right) \right]^{1/2}, \quad (19)$$

still limited by the small parameter $1/\kappa\tau \ll 1$. The CPMG signal is limited because Purcell decay is always active, while coherence is only transferred from the qubit to the transmission line for a small fraction of the time $\sim T_2^*/\tau \ll 1$. Since the times $t = n\tau$ of the revivals are known, we can improve on this limit if the coupling $g = g(t)$ or the detuning $\delta = \delta(t)$ is pulsed to eliminate Purcell decay for $|t - n\tau| \gtrsim T_2^*$. In this

case, we find a maximum achievable signal

$$S \lesssim S_{\text{max}} = \left(\frac{\kappa_2}{\kappa} \right)^{1/2} \quad (20)$$

that approaches $S_{\text{max}} \simeq 1$ for $\kappa_2 \simeq \kappa$ [29]. Transient spectroscopy can therefore achieve the same efficiency as a single-shot readout (one bit per cycle).

A central finding of this Letter is an even/odd modulation of echo revivals under dynamical decoupling. This modulation (a unique signature of quantum noise) results from the nonstationary analog of a Lamb shift arising from quantum fluctuations of an environment, an important indicator of nonclassical and non-Markovian dynamics [54,55]. When the correlation time of the environment is short compared to the typical observation time (Markovian limit), the quantum-noise phase $\Phi_q(t)$ will advance approximately linearly, $\Phi_q(t) \simeq \Delta\omega_{\text{Lamb}} t$, reflecting a simple frequency shift. In contrast, for a non-Markovian system, $\Phi_q(t)$ may have a highly nontrivial time dependence, reflecting a complex quantum dynamics. This phase may be amplified under repeated fast qubit rotations, which have the effect of stroboscopically driving the environment away from stationarity. Ignoring this effect during a quantum computation may then lead to an accumulation of phase errors that could otherwise be fully corrected.

Note added. Recently, we became aware of Ref. [56], which considers the influence of low-frequency qubit dephasing noise on the transient cavity transmission. In addition to the free-induction decay considered in Ref. [56], we also consider (i) dynamical decoupling sequences applied to the qubit, (ii) quantum noise, (iii) strategies for maximizing the signal, and (iv) cavity-induced backaction (an effect that is higher-order in g). As shown here, cavity-induced backaction ultimately sets the limiting timescale (determined by the inhomogeneously broadened Purcell decay time rather than by the cavity decay time $1/\kappa$) for monitoring qubit coherence through the cavity.

Acknowledgments. We thank A. Blais for useful discussions and Ł. Cywiński for both pointing out an error in our expression for the quantum filter function in an earlier manuscript and for bringing Refs. [41,42] to our attention. We also acknowledge funding from the Natural Sciences and Engineering Research Council (NSERC) and from the Fonds de Recherche–Nature et Technologies (FRQNT).

-
- [1] L. M. K. Vandersypen, H. Bluhm, J. S. Clarke, A. S. Dzurak, R. Ishihara, A. Morello, D. J. Reilly, L. R. Schreiber, and M. Veldhorst, Interfacing spin qubits in quantum dots and donors—hot, dense, and coherent, *npj Quantum Inf.* **3**, 34 (2017).
- [2] M. M. Desjardins, J. J. Viennot, M. C. Dartiailh, L. E. Bruhat, M. R. Delbecq, M. Lee, M.-S. Choi, A. Cottet, and T. Kontos, Observation of the frozen charge of a kondo resonance, *Nature* **545**, 71 (2017).
- [3] A. A. Clerk, K. W. Lehnert, P. Bertet, J. R. Petta, and Y. Nakamura, Hybrid quantum systems with circuit quantum electrodynamics, *Nat. Phys.* **16**, 257 (2020).

- [4] A. Stockklauser, P. Scarlino, J. V. Koski, S. Gasparinetti, C. K. Andersen, C. Reichl, W. Wegscheider, T. Ihn, K. Ensslin, and A. Wallraff, Strong Coupling Cavity QED with Gate-Defined Double Quantum Dots Enabled by a High Impedance Resonator, *Phys. Rev. X* **7**, 011030 (2017).
- [5] X. Mi, J. V. Cady, D. M. Zajac, P. W. Deelman, and J. R. Petta, Strong coupling of a single electron in silicon to a microwave photon, *Science* **355**, 156 (2017).
- [6] X. Mi, M. Benito, S. Putz, D. M. Zajac, J. M. Taylor, G. Burkard, and J. R. Petta, A coherent spin-photon interface in silicon, *Nature* **555**, 599 (2018).

- [7] N. Samkharadze, G. Zheng, N. Kalhor, D. Brousse, A. Sammak, U. C. Mendes, A. Blais, G. Scappucci, and L. M. K. Vandersypen, Strong spin-photon coupling in silicon, *Science* **359**, 1123 (2018).
- [8] A. J. Landig, J. V. Koski, P. Scarlino, U. C. Mendes, A. Blais, C. Reichl, W. Wegscheider, A. Wallraff, K. Ensslin, and T. Ihn, Coherent spin-photon coupling using a resonant exchange qubit, *Nature* **560**, 179 (2018).
- [9] T. Cubaynes, M. R. Delbecq, M. C. Dartiailh, R. Assouly, M. M. Desjardins, L. C. Contamin, L. E. Bruhat, Z. Leghtas, F. Mallet, A. Cottet, and T. Kontos, Highly coherent spin states in carbon nanotubes coupled to cavity photons, *npj Quantum Inf.* **5**, 47 (2019).
- [10] J. J. Viennot, M. C. Dartiailh, A. Cottet, and T. Kontos, Coherent coupling of a single spin to microwave cavity photons, *Science* **349**, 408 (2015).
- [11] D. J. van Woerkom, P. Scarlino, J. H. Ungerer, C. Müller, J. V. Koski, A. J. Landig, C. Reichl, W. Wegscheider, T. Ihn, K. Ensslin, and A. Wallraff, Microwave Photon-Mediated Interactions between Semiconductor Qubits, *Phys. Rev. X* **8**, 041018 (2018).
- [12] F. Borjans, X. G. Croot, X. Mi, M. J. Gullans, and J. R. Petta, Resonant microwave-mediated interactions between distant electron spins, *Nature* **577**, 195 (2020).
- [13] P. Harvey-Collard, J. Dijkema, G. Zheng, A. Sammak, G. Scappucci, and L. M. K. Vandersypen, Circuit Quantum Electrodynamics with Two Remote Electron Spins, *Phys. Rev. X* **12**, 021026 (2022).
- [14] C. J. Hood, M. S. Chapman, T. W. Lynn, and H. J. Kimble, Real-Time Cavity QED with Single Atoms, *Phys. Rev. Lett.* **80**, 4157 (1998).
- [15] J. Ye, D. W. Vernooy, and H. J. Kimble, Trapping of Single Atoms in Cavity QED, *Phys. Rev. Lett.* **83**, 4987 (1999).
- [16] A. Blais, A. L. Grimsmo, S. M. Girvin, and A. Wallraff, Circuit quantum electrodynamics, *Rev. Mod. Phys.* **93**, 025005 (2021).
- [17] C. W. Gardiner and M. J. Collett, Input and output in damped quantum systems: Quantum stochastic differential equations and the master equation, *Phys. Rev. A* **31**, 3761 (1985).
- [18] K. Jacobs, *Quantum Measurement Theory and its Applications* (Cambridge University Press, UK, 2014).
- [19] G. Burkard, M. J. Gullans, X. Mi, and J. R. Petta, Superconductor–semiconductor hybrid-circuit quantum electrodynamics, *Nat. Rev. Phys.* **2**, 129 (2020).
- [20] S. Schlör, J. Lisenfeld, C. Müller, A. Bilmes, A. Schneider, D. P. Pappas, A. V. Ustinov, and M. Weides, Correlating Decoherence in Transmon Qubits: Low Frequency Noise by Single Fluctuators, *Phys. Rev. Lett.* **123**, 190502 (2019).
- [21] J. J. Burnett, A. Bengtsson, M. Scigliuzzo, D. Niepce, M. Kudra, P. Delsing, and J. Bylander, Decoherence benchmarking of superconducting qubits, *npj Quantum Inf.* **5**, 54 (2019).
- [22] V. Ranjan, S. Probst, B. Albanese, A. Doll, O. Jacquot, E. Flurin, R. Heeres, D. Vion, D. Esteve, J. J. L. Morton, and P. Bertet, Pulsed electron spin resonance spectroscopy in the Purcell regime, *J. Magn. Reson.* **310**, 106662 (2020).
- [23] M. Le Dantec, M. Rančić, S. Lin, E. Billaud, V. Ranjan, D. Flanigan, S. Bertaina, T. Chanière, P. Goldner, A. Erb *et al.*, Twenty-three–millisecond electron spin coherence of erbium ions in a natural-abundance crystal, *Sci. Adv.* **7**, eabj9786 (2021).
- [24] O. Černotík, A. Dantan, and C. Genes, Cavity Quantum Electrodynamics with Frequency-Dependent Reflectors, *Phys. Rev. Lett.* **122**, 243601 (2019).
- [25] M. Bundgaard-Nielsen, J. Mørk, and E. V. Denning, Non-Markovian perturbation theories for phonon effects in strong-coupling cavity quantum electrodynamics, *Phys. Rev. B* **103**, 235309 (2021).
- [26] A. Carmele and S. Reitzenstein, Non-Markovian features in semiconductor quantum optics: quantifying the role of phonons in experiment and theory, *Nanophotonics* **8**, 655 (2019).
- [27] K. Sinha, P. Meystre, E. A. Goldschmidt, F. K. Fatemi, S. L. Rolston, and P. Solano, Non-Markovian Collective Emission from Macroscopically Separated Emitters, *Phys. Rev. Lett.* **124**, 043603 (2020).
- [28] D. O. Krimer, S. Putz, J. Majer, and S. Rotter, Non-Markovian dynamics of a single-mode cavity strongly coupled to an inhomogeneously broadened spin ensemble, *Phys. Rev. A* **90**, 043852 (2014).
- [29] See Supplemental Material at <http://link.aps.org/supplemental/10.1103/PhysRevResearch.4.L042039> for detailed derivations of the results presented in the main text.
- [30] F. Beaudoin and W. A. Coish, Enhanced hyperfine-induced spin dephasing in a magnetic-field gradient, *Phys. Rev. B* **88**, 085320 (2013).
- [31] L. M. Norris, G. A. Paz-Silva, and L. Viola, Qubit Noise Spectroscopy for Non-Gaussian Dephasing Environments, *Phys. Rev. Lett.* **116**, 150503 (2016).
- [32] Ł. Cywiński, R. M. Lutchyn, C. P. Nave, and S. Das Sarma, How to enhance dephasing time in superconducting qubits, *Phys. Rev. B* **77**, 174509 (2008).
- [33] U. Gavish, Y. Levinson, and Y. Imry, Detection of quantum noise, *Phys. Rev. B* **62**, R10637 (2000).
- [34] N. Zhao, J. Honert, B. Schmid, M. Klas, J. Isoya, M. Markham, D. Twitchen, F. Jelezko, R.-B. Liu, H. Fedder, and J. Wrachtrup, Sensing single remote nuclear spins, *Nat. Nanotechnol.* **7**, 657 (2012).
- [35] G. A. Álvarez and D. Suter, Measuring the Spectrum of Colored Noise by Dynamical Decoupling, *Phys. Rev. Lett.* **107**, 230501 (2011).
- [36] T. Yuge, S. Sasaki, and Y. Hirayama, Measurement of the Noise Spectrum Using a Multiple-Pulse Sequence, *Phys. Rev. Lett.* **107**, 170504 (2011).
- [37] J. Bylander, S. Gustavsson, F. Yan, F. Yoshihara, K. Harrabi, G. Fitch, D. G. Cory, Y. Nakamura, J.-S. Tsai, and W. D. Oliver, Noise spectroscopy through dynamical decoupling with a superconducting flux qubit, *Nat. Phys.* **7**, 565 (2011).
- [38] P. Szańkowski, G. Ramon, J. Krzywda, D. Kwiatkowski, and Ł. Cywiński, Environmental noise spectroscopy with qubits subjected to dynamical decoupling, *J. Phys.: Condens. Matter* **29**, 333001 (2017).
- [39] P. Szańkowski, Transition between continuous and discrete spectra in dynamical-decoupling noise spectroscopy, *Phys. Rev. A* **100**, 052115 (2019).
- [40] K. W. Chan, W. Huang, C. H. Yang, J. C. C. Hwang, B. Hensen, T. Tanttu, F. E. Hudson, K. M. Itoh, A. Laucht, A. Morello, and A. S. Dzurak, Assessment of a Silicon Quantum Dot Spin

- Qubit Environment via Noise Spectroscopy, *Phys. Rev. Appl.* **10**, 044017 (2018).
- [41] G. A. Paz-Silva, L. M. Norris, and L. Viola, Multiqubit spectroscopy of Gaussian quantum noise, *Phys. Rev. A* **95**, 022121 (2017).
- [42] D. Kwiatkowski, P. Szańkowski, and Ł. Cywiński, Influence of nuclear spin polarization on the spin-echo signal of an NV-center qubit, *Phys. Rev. B* **101**, 155412 (2020).
- [43] B. Hensen, W. W. Huang, C.-H. Yang, K. W. Chan, J. Yoneda, T. Tantt, F. E. Hudson, A. Laucht, K. M. Itoh, T. D. Ladd, A. Morello, and A. S. Dzurak, A silicon quantum-dot-coupled nuclear spin, *Nat. Nanotechnol.* **15**, 13 (2020).
- [44] F. Beaudoin, D. Lachance-Quirion, W. A. Coish, and M. Pioro-Ladrière, Coupling a single electron spin to a microwave resonator: controlling transverse and longitudinal couplings, *Nanotechnology* **27**, 464003 (2016).
- [45] A. Shnirman, G. Schön, I. Martin, and Y. Makhlin, Low- and High-Frequency Noise from Coherent Two-Level Systems, *Phys. Rev. Lett.* **94**, 127002 (2005).
- [46] Y. M. Galperin, B. L. Altshuler, J. Bergli, and D. V. Shantsev, Non-Gaussian Low-Frequency Noise as a Source of Qubit Decoherence, *Phys. Rev. Lett.* **96**, 097009 (2006).
- [47] R. Zhao, T. Tantt, K. Y. Tan, B. Hensen, K. W. Chan, J. C. C. Hwang, R. C. C. Leon, C. H. Yang, W. Gilbert, F. E. Hudson, K. M. Itoh, A. A. Kiselev, T. D. Ladd, A. Morello, A. Laucht, and A. S. Dzurak, Single-spin qubits in isotopically enriched silicon at low magnetic field, *Nat. Commun.* **10**, 5500 (2019).
- [48] F. K. Malinowski, F. Martins, P. D. Nissen, E. Barnes, Ł. Cywiński, M. S. Rudner, S. Fallahi, C. Gardner, Geoffrey, M. J. Manfra, C. M. Marcus, and F. Kuemmeth, Notch filtering the nuclear environment of a spin qubit, *Nat. Nanotechnol.* **12**, 16 (2017).
- [49] J. Mielke, J. R. Petta, and G. Burkard, Nuclear spin readout in a cavity-coupled hybrid quantum dot-donor system, *PRX Quantum* **2**, 020347 (2021).
- [50] For $h(t) = e^{i(H_E - h/2)t} h e^{-i(H_E - h/2)t} = \sum_{\alpha} c_{\alpha}(t) I_{\alpha}$, the quantum-noise term produces a phase arising from $\langle [h(t), h] \rangle = i \sum_{\alpha\beta} \epsilon_{\alpha\beta\gamma} c_{\alpha}(t) c_{\beta}(0) \langle I_{\gamma} \rangle$, which is nonzero for a polarized initial state, $\langle I_{\gamma} \rangle = \text{Tr}(\hat{\rho}_E I_{\gamma}) \neq 0$. This analysis applies within the Gaussian approximation, which can be justified even for a single spin at short times.
- [51] J. M. Taylor, P. Cappellaro, L. Childress, L. Jiang, D. Budker, P. Hemmer, A. Yacoby, R. Walsworth, and M. Lukin, High-sensitivity diamond magnetometer with nanoscale resolution, *Nat. Phys.* **4**, 810 (2008).
- [52] J. Gambetta, A. Blais, D. I. Schuster, A. Wallraff, L. Frunzio, J. Majer, M. H. Devoret, S. M. Girvin, and R. J. Schoelkopf, Qubit-photon interactions in a cavity: Measurement-induced dephasing and number splitting, *Phys. Rev. A* **74**, 042318 (2006).
- [53] A. N. Korotkov, Quantum Bayesian approach to circuit QED measurement with moderate bandwidth, *Phys. Rev. A* **94**, 042326 (2016).
- [54] D. P. DiVincenzo and D. Loss, Rigorous born approximation and beyond for the spin-boson model, *Phys. Rev. B* **71**, 035318 (2005).
- [55] W. A. Coish, J. Fischer, and D. Loss, Free-induction decay and envelope modulations in a narrowed nuclear spin bath, *Phys. Rev. B* **81**, 165315 (2010).
- [56] P. M. Mutter and G. Burkard, Fingerprints of Qubit Noise in Transient Cavity Transmission, *Phys. Rev. Lett.* **128**, 236801 (2022).